142 CONVECTIVELY-INDUCED SEVERE WIND GUSTS IN SOUTHERN BRAZIL: SURFACE OBSERVATIONS, ATMOSPHERIC ENVIRONMENT, AND ASSOCIATION WITH DISTINCT CONVECTIVE MODES

Vanessa Ferreira[1]*, and Ernani L. Nascimento[1]
[1]Grupo de Modelagem Atmosférica, Universidade Federal de Santa Maria, Santa Maria/RS, Brazil

1. INTRODUCTION

Subtropical South America is recognized as one of the world's most active regions for severe convective storms (Brooks 2006; Zipser et al. 2006; Cecil and Blankenship 2012), with damaging winds being one of the phenomena that these storms can generate. While an extensive scientific literature exists addressing the documentation and understanding of intense convectively-generated wind gusts in North America (Johns and Hirt 1987; Mueller and Carbone 1987; Atkins and Wakimoto 1991; Wakimoto 2001) equivalent investigations in South America are still scarce. Particularly in Brazil, the climatology of wind gusts produced by severe thunderstorms is still poorly documented, despite the high social and economic impact of such occurrences (Reckziegel, 2007).

The goal of this study is to investigate the occurrence and to generate a short climatology of severe wind gusts (SWGs; gust speeds equal to or above 25 ms^{-1}) detected by surface hourly data from the operational network of automated weather stations (AWSs) located in southern Brazil and operated by Brazil´s National Meteorological Institute (INMET, in portuguese). Only those events unequivocally associated with deep convective storms were selected, comprising the period from 2005 to 2015.

The temporal and spatial distributions of the SWGs were studied, and an effort was made to characterize the atmospheric environment in which a few of the SWGs developed utilizing available proximity soundings. The prevailing convective modes that generated the SWGs were analyzed for the situations when radar data were available. We also assessed the capability of INMET's AWS synoptic network to detect convectively-induced surface features that are closely associated with gust fronts, such as surface cold pools and mesohighs.

* *Corresponding author address:* Vanessa Ferreira, Dept. Física, Universidade Federal de Santa Maria, Santa Maria/RS, CEP.97105-900, Brazil; email: assenavmet@gmail.com.

2. DATA AND METHODOLOGY

For this study, hourly meteorological data were obtained from 94 INMET's AWSs located in a geographical domain that comprises the three states of Brazil's south (Paraná, Santa Catarina and Rio Grande do Sul) and southern portions of São Paulo and Mato Grosso do Sul states (Figure 1). This sector was selected because is placed within the area of most frequent occurrence of severe convective storms in Brazil (Nascimento, 2005). INMET's AWSs provide hourly measurements of the strongest 3-second wind gust (at 10 m AGL) recorded in the 60 min interval that precedes the time of the automated weather report, which is regularly at the top of each hour; however, no information about the ***exact*** time of the strongest wind gust is provided. The period of study spanned from 1 January 2005 to 31 December 2015.

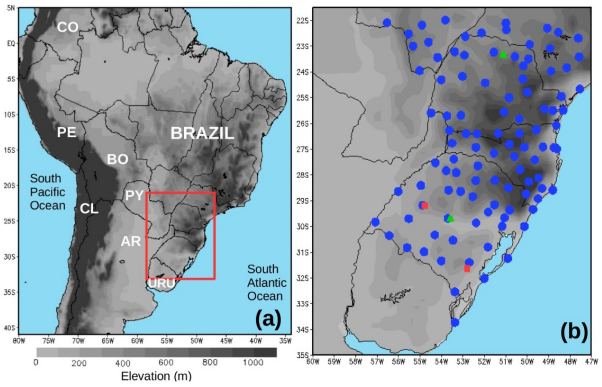

Figure 1: (a) Geographical domain of interest. (b) Spatial distribution of INMET's operational network of surface AWS (blue circles); location of Santiago (SNTG) and Canguçu (CNGÇ) S-band Doppler radars (red retangles); location of Santa Maria (SBSM) and Londrina (SBLO) upper-air stations.

First, a threshold of 25 ms^{-1} was utilized to characterize a wind gust as “severe” (SWG). Next, to discriminate only those SWGs associated with deep convective storms (hence, characterizing a ***severe convective storm***; Moller 2001), thermal infrared imagery from the Geostationary Operational Environmental Satellite (GOES-12 and GOES-13) was analyzed for the location of

the AWS in order to certify that deep convection was in place over the station around the time of the SWG report. If a convective storm displaying top with brightness temperature equal to or less than -55°C was present over the AWS within a +/-1 hour window around the report of the SWG then the event advanced to the next step of the screening. The next criterion for selection consisted of the occurrence of 1-hr rainfall accumulation of at least 1 mm in the AWS within the same hour in which the SWG was detected.

In the sample of wind gusts that suited all the aforementioned criteria, a number of episodes suspicious of not being of convective origin persisted. All of these were observed among four AWSs, two of which located at high elevation (above 1200 m), and two others located in coastal sectors that are well known for the frequent occurrence of extratropical cylones in southern Brazil. These suspicious reports consisted of SWGs persisting for several hours, which is not consistent with the behavior of local convective storms. The study by Ferreira and Nascimento 2015, that evaluated these episodes in detail using a more subjective approach, showed that these suspicious reports of SWGs were not unequivocally associated with local convective storms, but with either: (i) a 850hPa low-level-jet-like flow impinging directly at the surface, for the AWSs located on higher elevation; or (ii) the presence of an extratropical cyclone just off the coast of southern Brazil, for the two coastal AWSs. The suspicious events were, therefore, excluded from the sample of SWGs, except for eight episodes that were confirmed as from convective origin by the subjective analysis.

Once concluded the sampling of convectively-induced SWGs, absolute frequency distributions on diurnal and seasonal scales were produced, as well as a map of the spatial distribution of the SWGs.

Hourly time-series of station-level atmospheric pressure, rainfall accumulation, and air temperature and dew points at 2 m AGL for an interval of +/-10 h around the time of the SWG reports were also studied. This was carried out with the objective to investigate the mean temporal behavior of surface variables preceding and after the occurrence of a SWG. (It must be mentioned that INMET´s AWSs report not only the scalar variables valid at the top of each hour but also the minimum and maximum values of these variables observed in the 60 min period that precedes each report; but, as for the hourly maximum wind gust, no information is provided regarding the exact time of occurrence of the minimum/maximum values).

In order to factor out the effects of distinct station elevations upon pressure and temperature values, the variations of these variables (at the top of each hour) were analyzed not in terms of their absolute reported values, but in terms of their hourly deviations from the corresponding mean values for the +/-10 h time window. These hourly deviations were then averaged for all SWG events leading to hourly time series of mean deviations of pressure and temperature with respect to the mean values of the full +/-10 h interval.

To assess the capability of INMET´s AWS network to detect surface mesoscale features typically associated with convectively-induced gust fronts (namely, cold pools and mesohighs), emphasis was given to the characterization of temperature decrease and pressure increase around the time the SWG was reported. Magnitudes of the variation in temperature (ΔT) and pressure (ΔP) were calculated for each event using the absolute difference between the overall maximum and overall minimum values of these variables reported in the time interval between the hour of the SWG report and 1 h later. This procedure was employed to ***assess*** the magnitude of the surface cold pools and mesohighs, following a similar approach utilized by Engerer et al. 2008.

It is important to stress that we extended the time interval for computing ΔT and ΔP to 1 h after the reporting time of the SWG because there is no information available from INMET's AWS about the exact time of occurrence of the SWG. Thus, keeping the screening period to only within the hour of the SWG report could be inadequate to estimate the magnitude of ΔT and ΔP induced by the convective activity.

For the AWSs located in Rio Grande do Sul (RS) state, base reflectivity and Doppler velocities from weather radars operated by the Brazilian Air Force were utilized to identify the main convective mode of the storms that produced the SWGs. In RS, these S-band (10-cm wavelength) single-polarization Doppler radars are (see Figure 1): Santiago (SNTG), located in the mid-western section of the state (29°13′30″S; 54°55′48″ W; elevation: 434 m), and Canguçu (CNGÇ), in southeastern RS (31°24'14"S; 52°42'06"W; elevation: 466 m). In short pulse mode they operate with a range of 250 km and pulse repetition frequency of 600 Hz, with a beam-width of approximately 2°. In volume scan mode they perform a full set of plan position indicators (PPIs) for 15 elevations at 10 min intervals. Post-processing of the raw radar data was conducted using PyART (Collis and Helmus 2015).

Finally, the local observed atmospheric conditions during the SWGs were studied for four cases in which available upper-air observations met the criteria for a proximity sounding, as defined by Brooks et al. 1994. In this study, however, we slightly modified these criteria to allow for soundings performed as early as three hours before the SWG report. These soundings, obtained from the Wyoming Weather Web of the University of Wyoming's Department of Atmospheric Science, were analyzed in skew-T diagrams and through the computation of several parameters that describe the magnitude of conditional instability, vertical wind shear in distinct layers, and moisture availability. This was carried out utilizing the SHARPpy algorithm (Halbert et al. 2015) fully adapted to the Southern Hemisphere. Additionally, the predictive skill of the parameters WINDEX (McCann 1994), GUSTEX (Geerts 2001), and modified GUSTEX (Dotzek and Friedrich 2008) was evaluated for these four profiles.

3. RESULTS

3.1. Seasonal, diurnal and spatial distribution

After following the procedures described in the previous section, a total of 250 convectively-generated SWGs (henceforth referred to as simply "SWG") were identified between January 2005 and December 2015. Figure 2a shows that the highest frequency of SWGs in southern Brazil was in the (austral) Spring and Summer months, which is consistent with findings from studies that address the climatology of severe convective storms in the La Plata Basin (LPB) using remote sensing techniques (e.g., Cecil and Blankenship 2012). Most SWGs were detected from mid-afternoon to late evening hours, with a secondary peak in the overnight hours (Fig.2b; LST = UTC-3h). Fewer events were identified during the morning. This result agrees with the diurnal variation of convective activity in southern Brazil.

Overall, the western portion of Brazil's south displayed the largest frequency of SWGs in our sample (Fig. 3). This result suggests two main things: first, nocturnal mesoscale convective systems (MCSs) that commonly form over central-northeastern Argentina and cross the border with Brazil may be the source for many of such SWG events; second, a role played by the synoptic-scale northern Argentina (inverted) trough that often extends into western sections of southern Brazil (with an attending northwesterly low-level jet stream) in setting up the environment for the development of severe thunderstorms.

Furthermore, this result is also in agreement with climatological studies which show that the highest frequency of severe storms in the LPB occur over northeastern Argentina reducing gradually toward the brazilian south, while maintaining a relatively high frequency over Brazil (Cecil and Blankenship 2012; Brooks 2006).

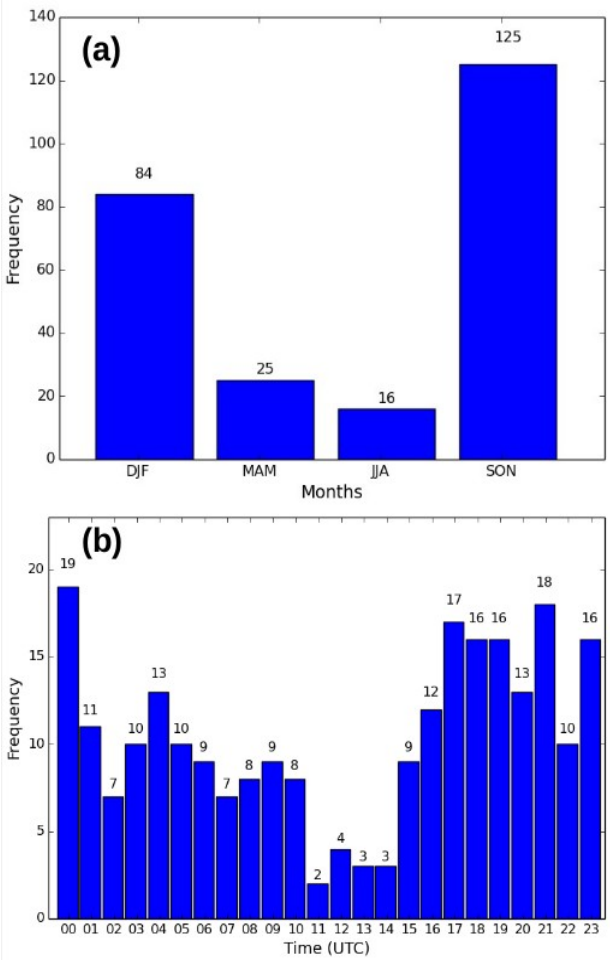

Figure 2: Absolute frequencies of SWGs detected by INMET's AWS network for the 2005-2015 period in southern Brazil: (a) seasonal distribution (DJF: Summer; MAM: Fall; JJA: Winter; SOM: Spring); (b) hourly distribution (local standard time = UTC-3h).

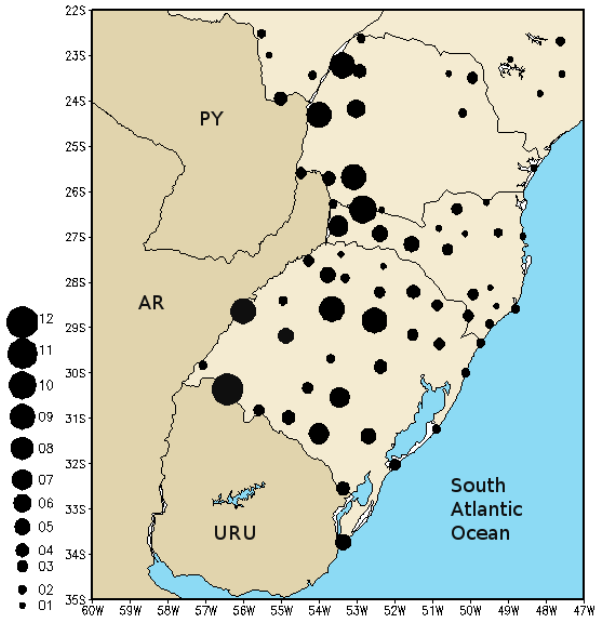

Figure 3: Total number os SWGs detected by INMET's AWS network from January 2005 to December 2015. The diameters of the circles are proportional to the number of events.

3.2. Hourly time series and statistics.

Figure 4 shows hourly time series of strongest 3 s wind gust and 1hr-accumulated rainfall averaged for all the 250 SWG events for a 20 h time window centered at the reporting time of the SWGs (hour 0). These time series shows an isolated peak at hour 0 for both rainfall and maximum gust, highlighting the short-lived behavior of the meteorological event, which is typical of local convection. This result also confirms the suitability of the set of criteria and procedures used in this study to identify strong wind gusts associated with local convective storms, rather than with long-lived weather systems (e.g., extratropical cyclones).

Figure 5 displays hourly time series of mean anomalies for (a) atmospheric pressure and (b) temperature with respect to the corresponding mean values over the 20 h time window, averaged for the 250 SWGs. In terms of time tendency of the pressure anomalies, there was a well defined change from negative, several hours prior the to the SWG, to strongly positive ***at*** the time of the SWG, followed by positive anomalies in the hours following the SWG.

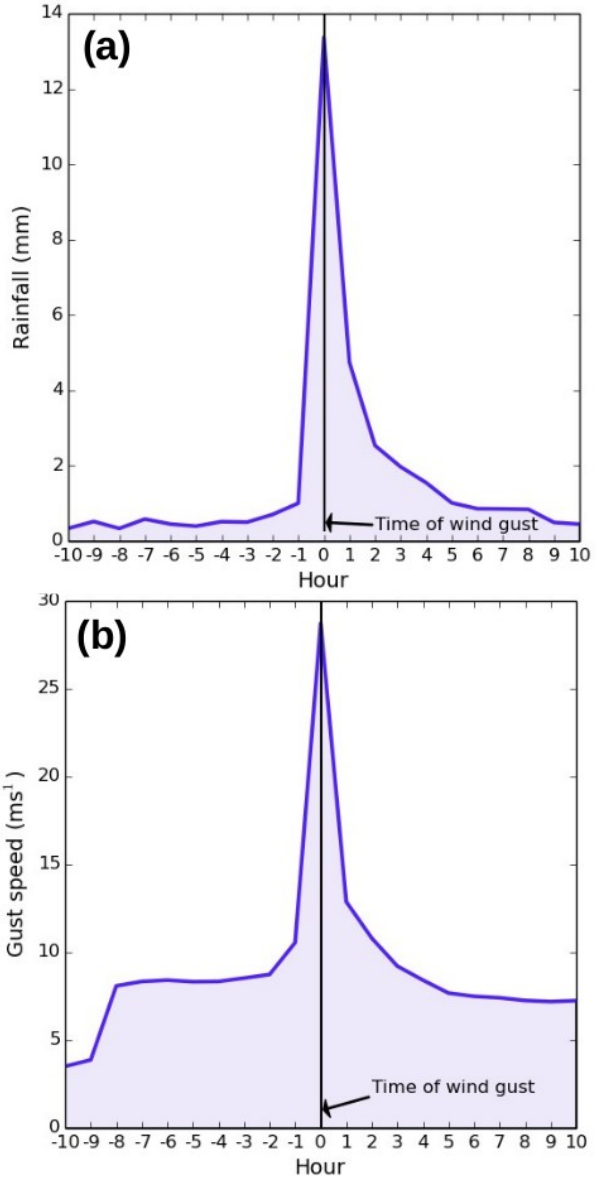

Figure 4: Hourly time series of (a) strongest 3 s wind gust and (b) 1-hr accumulated rainfall, averaged for the 250 SWGs for a +/-10 hour time window around the SWG report. (The arrow at hour 0 indicates the time of the hourly wind gust report that corresponds to the SWG, not the exact instant of the SWG, which is unknown).

A closer inspection in a shorter time interval around the SWG report, shows, in average, a slight increase in pressure in the hour preceding the SWG report followed by a sharp increase within the 1 hour interval in which the SWG was recorded (Fig. 5a). It is in this 1 hour interval that the largest positive tendency in pressure (in fact, the largest pressure tendency regardless of the sign) was found, and when the sign of the mean pressure anomaly swapped from negative to

positive. In the hours following the SWG, pressure variations displayed weaker positive tendency. In other words, the SWGs were accompanied by a short lived “pressure jump” followed by a slow-evolving increase in pressure. This short-lived pressure perturbation is consistent with the manifestation of a surface mesohigh, even though the finescale temporal variation of this feature remained undetectable by the hourly reports from INMET´s AWSs.

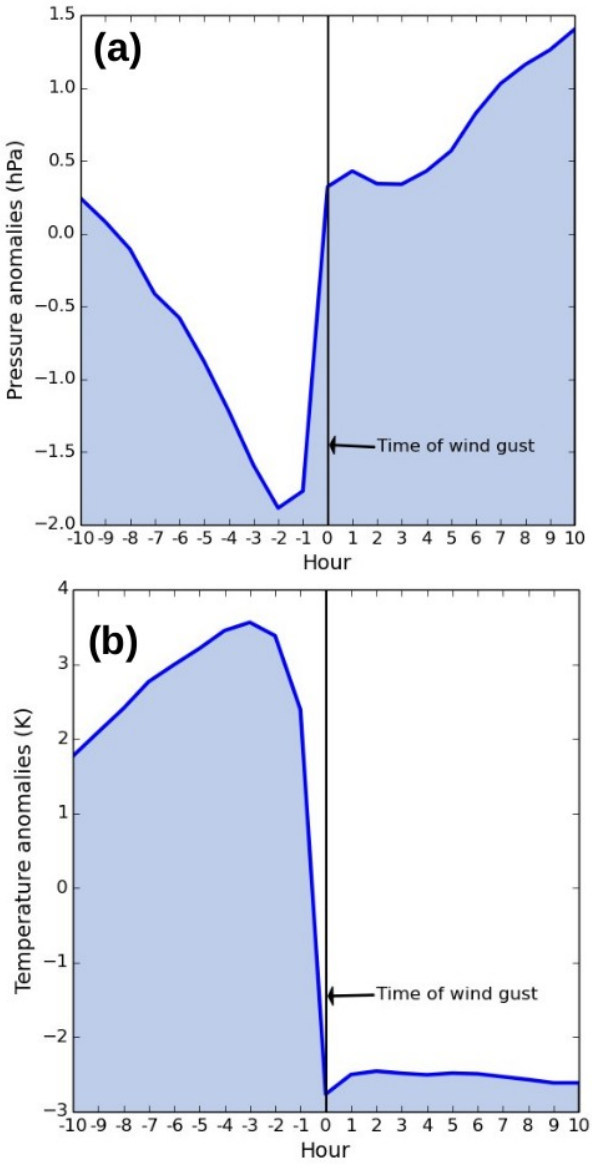

Figure 5: Hourly time series of mean anomalies of (a) atmospheric pressure (hPa) and (b) air temperature (K) with respect to their corresponding mean values over the +/-10 hour time window around the SWG report, averaged for 250 SWGs. (The arrow at hour 0 indicates the time of the hourly wind gust report that corresponds to the SWG, not the exact instant of the SWG, which is unknown).

Regarding air temperature (Fig. 5b), the time series of mean anomalies shows a change from positive anomalies prior to the SWG to negative anomalies following the SWG. Again, it is within the 1 hour interval of the SWG report that the largest time tendency was observed, and with the sign of the temperature anomaly changing from positive to negative. This behavior coincides with that described for the pressure anomalies, but with reversed signs. This finding is no surprise since mesohighs are (mostly) a hydrostatic response to the presence of the convectively-induced cold pool.

In summary, the variations in temperature and pressure anomalies found for the hour in which the SWGs were reported were much sharper than the synoptic-scale evolution of these variables for the hours preceding and following the SWGs.

Figure 6 shows the quantile distribution, for the 250 SWGs, of the absolute variations in atmospheric pressure (ΔP), air temperature (ΔT) and dew points (ΔDWP) in a time interval spanning from the 1-hr period of the SWG report and 1 hours later (i.e., from hour 0 to hour 1 in Figs. 4 and 5, following the methodology described in the previous section). As expected, pressure [temperature] variations were positive [negative] in all events, consistent with the manifestation of surface mesohighs and cold pools discussed earlier. The median value of ΔP was +3.5 hPa, with highest value reaching +8.2 hPa. The median value for ΔT was -6.1 K, with the strongest drop being -17.4 K. Dew point variations displayed a behavior similar to ΔT, with a median of -3.5 K and strongest drop of -8.6 K. The magnitudes of ΔP and ΔT are of the same order of magnitude of those reported in other studies (Engerer et al. 2008; Provod et al. 2015).

3.3. Classification of convective modes

Among the 250 SWG events, base reflectivity fields from nearby S-band weather radars were available for 30 episodes. These were utilized to identify the (main) convective mode of the storms that produced the SWGs. Following Gallus et al. 2008, convective modes were classified as individual cells, multicell clusters, linear MCSs (i.e., squall lines/bow echoes), and nonlinear MCSs. Figure 7 depicts examples for each convective mode.

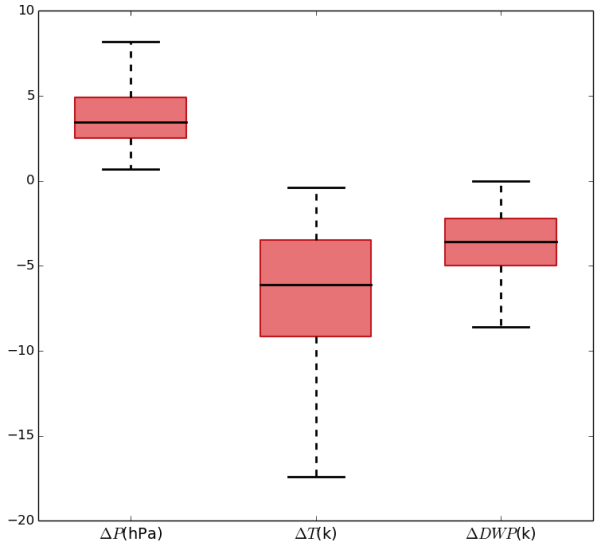

Figure 6: Boxplots of the quantile distribution of variations in pressure (ΔP, in hPa), temperature (ΔT, in K) and dew point (ΔDWP, in K) for the 250 SWGs in a time interval from hour 0 to hour 2 (see Figs. 3 and 4). Boxes indicate the interval between the 25th to 75th percentiles, whiskers are the 5th and 95th percentiles, and the horizontal line in each box indicates the median value.

Only one SWG event was associated with an individual cell, while seven were associated with multicell cluster, three with nonlinear MCS, and nineteen with linear MCS. In a first analysis, this finding strongly suggests that a large number of SWGs over southern Brazil are generated by squall lines. However, this result may also reflect the greater likelihood of a network of AWSs in detecting more widespread SWGs associated with larger (and longer-lived) convective systems.

3.4. Atmospheric profiles

For only four cases out of the 250 SWG events were there available upper-air observations in the vicinities of the AWS that met all the criteria for a proximity sounding. As expected, the vertical profiles from these soundings revealed a conditionally unstable environment (Fig.8), with surface-based [most unstable] CAPE ranging from 130 J kg^{-1} to 2011 J kg^{-1} [1540 to 2609 J kg^{-1}], and downdraft CAPE (DCAPE) ranging from 600 J kg^{-1} to 1685 J kg^{-1}. The unstable environments (Fig. 8) were characterized by mid-level lapse rates (MLLRs) that were not particularly strong, varying from 5.2 K km^{-1} to 6.8 K km^{-1} (the 75th percentile for MLLR in the LPB is 6.78 K km^{-1}; Nascimento et al. 2016), but by moderately steep 0-3km lapse rates (LLLRs), varying from 5.2 K km^{-1} to 7.5 K km^{-1} (the 75th percentile for LLLR in the LPB is 6.16 K km^{-1}; Nascimento et al. 2016).

Deep layer vertical wind shear varied considerably among the proximity soundings. The sounding with weakest bulk wind shear for both 0-3km and 0-6km layers (Fig. 8a) displayed a large theta-e index (TEI; defined as the difference between the surface theta-e and the minimum theta-e in the lowest 400hPa AGL; Atkins and Wakimoto 1991) of 28 K and very strong DCAPE (1393 J kg^{-1}). Just for comparison, the 90th percentile for TEI [95th percentile for DCAPE] in the LPB is 29 K [1286 J kg^{-1}] (Nascimento et al. 2016); this suggests that the thermodynamic forcing prevailed over vertical momentum transport in generating the SWG in that case. Conversely, the sounding with strongest 0-6 km bulk wind shear (32 ms^{-1}), which also displayed an intense 0-3km bulk shear of 23 ms^{-1} (Fig. 8c) showed a substantially lower TEI (16 K, which is below the median value of 19 K for TEI in the LPB; Nascimento et al. 2016), indicating a more prominent role played by the vertical momentum transport in generating strong downdrafts.

Interestingly, the strongest SWG considering the four cases (11 December 2012) was associated with the profile with highest TEI (32 K, equal to the 95th percentile for TEI in the LPB; Nascimento et al. 2016; Fig. 8b), highest DCAPE (1685 J kg^{-1}, which is well above the 95th percentile for DCAPE in the LPB), and steepest LLLR (7.5 K km^{-1}, above the 95th percentile for LLLR in the LPB) among the four soundings, while at the same time displaying moderately strong deep layer shear (28 ms^{-1}, above the 90th percentile for the LPB; Nascimento et al. 2016). This finding suggests that both the thermodynamic forcing and the vertical momentum transport played a role in generating that SWG.

Wind gust estimations using WI, GU1 and GU2 parameters applied to the four proximity soundings are compared *vis-à-vis* to the observed SWGs in Table 1.

WI performed well for the 12 January 2010 episode and provided an almost perfect forecast for the 11 December 2012 event. This results from the combination of a strong 0-1km lapse rate (6.4 K km^{-1}) ***and*** low mixing ratio at the melting level (0.66 g kg^{-1}), which both drive a high value of WI. In contrast, a substantial underestimation of the wind gusts by WI was found in the 29 May 2013 and 02 January 2015 events. A possible explanation for this was both a weaker 0-1km lapse rate ***and*** a moister atmosphere at the

melting level. For the May event the 0-1km lapse rate was 5.4 K km^{-1} which, combined with a high mixing ratio at the melting level (4.80 g kg^{-1}), led to the underestimation of the wind gust. In the January episode, the 0-1km lapse-rate was slightly stronger (5.8 K km^{-1}), but with higher mixing ratio at the melting level (5.8 g kg^{-1}).

Table 1: SWGs detected by INMET´s AWS and the corresponding gust estimates using indices WI, GU1 and GU2 from the proximity soundings.

Proximity sounding	SWG (ms^{-1})	WI (ms^{-1})	GU1 (ms^{-1})	GU2 (ms^{-1})
12Z 12Jan2010	27.8	24.2	17.6	35.3
00Z 11Dec2012	29.3	29.6	31.7	46.7
12Z 29May2013	25.4	7.7	20.9	31.9
00Z 02Jan2015	27.3	16.8	20.9	39.2

Both GU1 and GU2 modify WI by incorporating the influence of vertical momentum transport from higher levels. To achieve that, GU1 includes in the formulation the wind speed at 500 hPa while GU2 utilizes the density-weighted mean wind between 1 and 5 km AGL. The vertical momentum transport is a factor contributing to high wind events at the ground, and generally gust strengths estimated by GU1 and GU2 are stronger than WI. However, for the 12 January 2010 event the wind gust computed by GU1 was much weaker than that predicted by WI (leading to a significant underestimation when compared to the observed wind gust). The bad performance by GU1 in this case resulted from weak winds at 500 hPa (12 ms^{1}). In contrast, in the presence of stronger winds aloft in the 29 May 2013 and 02 January 2015 events, GU1 improved considerably the wind gust estimation compared to WI, even though provided an underestimation when compared to the observation. On the other hand, GU2 significantly overestimated the gust speed for all the cases.

Given the few number of actual proximity soundings (precluding any statistically-significant result), future work will investigate atmospheric profiles extracted from reanalysis data at the nearest grid-points to the SWG reports.

4. SUMMARY AND FINAL REMARKS

Our study showed that it is possible to identify intense wind gusts associated with convective storms in Brazil applying a combined approach using data from INMET's AWS and thermal-infrared imagery from a geostationary meteorological satellite.

The highest frequency of SWGs was observed during the Spring months, followed by Summer. Most SWGs were detected from mid-afternoon to late evening, with a secondary peak in the overnight hours. Overall, the western portion of Brazil's south was the region with the highest number of SWGs.

The observed behavior of the thermodynamic variables during the SWG events was generally consistent with the conceptual model of convectively-driven cold pools (temperature drop) and mesohighs (pressure jump). The median value of pressure [temperature] variations accompanying the SWG was +3.5 hPa [-6.1 K], with a 95th percentile [5th percentile] of +8.2 hPa [-17.4 K]. These variations are comparable to the ones found in the literature for other regions in the world (e.g., Engerer et al. 2008).

Our results suggest that a large number of SWGs observed in southern Brazil are generated by squall lines, particularly in Rio Grande do Sul state, where radar data was available for this study. However, the few number of events with radar data analysis did not allow a representative conclusion on that matter.

Only four proximity soundings were found for the SWG events. The vertical profiles revealed a conditionally unstable environment, with DCAPE above its 75th [95th] percentile in three [two] soundings. In two profiles the TEI was high, around its respective 90th percentile for the LPB region. MLLRs were not particularly strong, whereas LLLRs were above its 75th percentile in three of the four soundings. At least one proximity sounding (00Z 11 December 2012) displayed extreme values of virtually all parameters considered important for driving strong downdrafts in convective storms. Deep layer vertical wind shear varied considerably among soundings.

Future work will expand the analysis of atmospheric profiles and pre-convective environments utilizing reanalysis data.

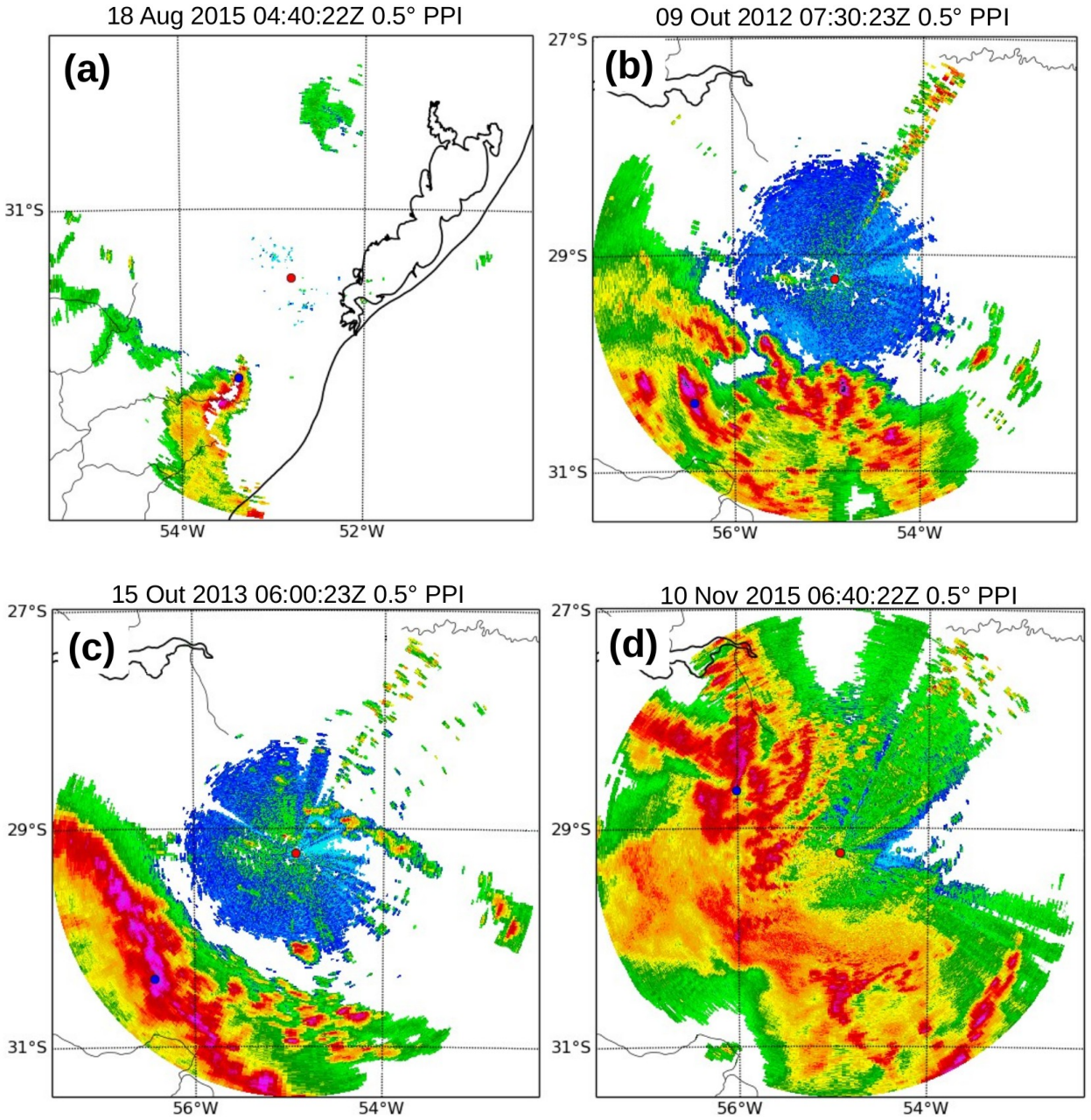

Figure 7: PPIs at 0.5° elevation of base reflectivity (dBZ) for four episodes of convective storms that generated SWG events identified in this study. Each panel exemplifies one class of convective mode: (a) individual cell (18 Aug 2015; CNGÇ radar); (b) multicell clusters (09 Oct 2012, SNTG radar); (c) linear MCS (15 Oct 2013, SNTG radar); (d) nonlinear MCS (10 Nov 2015, SNTG radar). The blue [red] dot in each panel indicates the location of the AWS [radar]. These images are the ones closest to the time of the respective SWG reports.

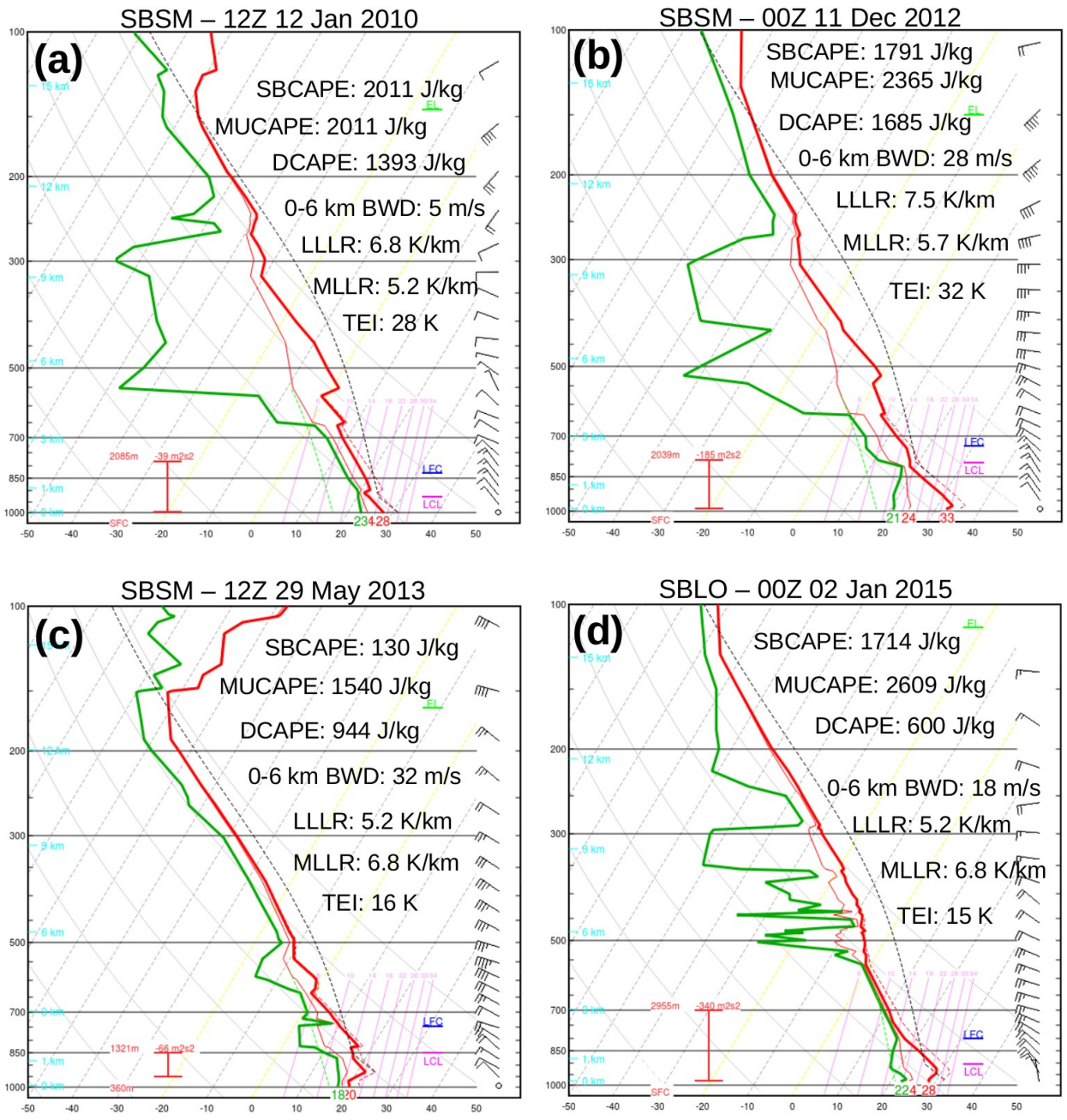

Figure 8: Proximity soundings for four SWG episodes: (a) Santa Maria (SBSM) sounding at 12Z 12 January 2010. (b) SBSM sounding at 00Z 11 December 2012. (c) SBSM sounding at 29 May 2013. (d) Londrina (SBLO) sounding at 00Z 02 January 2015.

6. ACKNOWLEDGMENTS

This study is part of the first author's Master's Degree research project, funded by Coordenação de Aperfeiçoamento de Pessoal de Nível Superior (CAPES). We would like to thank the Environmental Satellite Division from Brazil's National Space Research Institute (DSA-INPE), and in particular meteorologist Thiago Biscaro, for making available the raw radar data used in this study. We also thank INMET for making available the AWS data, and PyArt and SHARPpy developers. We also acknowledge the Graduate Program in Meteorology and the Department of Physics of the Federal University of Santa Maria for providing funding that partially covered the costs of the author's participation in the confrerence.

5. REFERENCES

Atkins, N. T., and R. M. Wakimoto, 1991: Wet microburst activity over the southeastern United States: Implications for forecasting. Weather and forecasting, v. 6, n. 4, p. 470-482, 1991.

Brooks, H. A global view of severe thunderstorms, 2006: Estimating the current distribution and possible future changes, preprints. In: AMS Severe Local Storms Special Symposium.

———, Doswell, C.A., Cooper, J., 1994. On the environments of tornadic and nontornadic mesocyclones. Weather and forecasting, v. 9, n. 4, p. 606-618.

Cecil, D. J., Blankenship, C. B., 2012: Toward a global climatology of severe hailstorms as estimated by satellite passive microwave imagers. Journal of Climate, v. 25, n. 2, p. 687–703.

Collis, S., and Helmus, J., 2015: Using the Scientific Python ecosystem to advance open radar science. 2015 AGU Fall Meeting.

Dotzek, Nikolai; Friedrich, Katja. Downburst-producing thunderstorms in southern Germany, 2009: Radar analysis and predictability. Atmospheric Research, v. 93, n. 1, p. 457-473.

Engerer, N. A.; Stensrud, D. J.; Coniglio, M. C., 2008: Surface characteristics of observed cold pools. Monthly Weather Review, v. 136, n. 12, p. 4839–4849.

Ferreira, V.; Nascimento, E. de L., 2015: Discriminação entre rajadas de vento convectivas e não-convectivas. Ciência e Natura.

Gallus JR, William A.; Snook, Nathan A.; Johnson, Elise V., 2008: Spring and summer severe weather reports over the Midwest as a function of convective mode: A preliminary study. Weather and Forecasting, v. 23, n. 1, p. 101-113.

Geerts, B., 2001. Estimating downburst-related maximum surface wind speeds by means of proximity soundings in New South Wales, Australia. Wea. Forecasting, 16, 261–269.

Halbert, K. T., W. G. Blumberg, and P. T. Marsh, 2015: "SHARPpy: Fueling the Python Cult". Preprints, 5th Symposium on Advances in Modeling and Analysis Using Python, Phoenix AZ.

Johns, R. H.; Hirt, W. D., 1987: Derechos: Widespread convectively induced windstorms. Weather and Forecasting, v. 2, n. 1, p. 32–49.

McCann, D. W., 1994: WINDEX-A new index for forecasting microburst potential. Wea. Forecasting, 9, 532–541.

Moller, A. R., 2001: Severe local storms forecasting. Meteorological Monographs, American Meteorological Society, v. 28, n. 50, p. 433–480.

Mueller, C. K.; CARBONE, R. E., 1987 Dynamics of a thunderstorm outflow. Journal of the atmospheric sciences, v. 44, n. 15, p. 1879–1898.

Nascimento, E. d. L., 2015: Previsão de tempestades severas utilizando-se parâmetros convectivos e modelos de mesoescala: uma estratégia operacional adotável no brasil. Revista Brasileira de Meteorologia, v. 20, n. 1, p. 121–140, 2005.

———, Foss, M., Ferreira. V., Brooks, H.; 2016: An updated and expanded climatology of severe weather parameters for Subtropical South America as derived from upper-air observations and CFSR-CFSv2 data. In: AMS 28th Conference on Severe Local Storms, Portland, OR.

Provod, M.; Marsham, J.; Parker, D.; Birch, C. E., 2015 A characterization of cold pools in the west african sahel. Monthly Weather Review, n. 2015.

Reckziegel, B., 2007: Levantamento dos desastres desencadeados por eventos naturais

adversos no estado do rio grande do sul no período e 1980 a 2005. Levantamento dos Desastres Desencadeados por Eventos Naturais Adversos no Estado do Rio Grande do Sul no Período de 1980 a 2005, v. 1.

Wakimoto, R. M., 2001: Convectively driven high wind events. Meteorological Monographs, v. 28, p. 255-298.

Zipser, E. J.; LIU, C.; CECIL, D. J.; Nesbitt, S. W.; Yorty, D. P., 2006: Where are the most intense intensethunderstorms on earth? Bulletin of the American Meteorological Society, v. 87, n. 8, p. 1057–1071.